V European Conference on Computational Fluid Dynamics
ECCOMAS CFD 2010
J. C. F. Pereira and A. Sequeira (Eds)
Lisbon, Portugal, 14–17 June 2010

# EFFECTS OF GEOMETRY MODIFICATION ON THE AERODYNAMICS OF A GENERIC BRIDGE DECK SECTION

**Daniel C. Vaz[*], Éric Didier[†], and António R. J. Borges[†]**

[*]Departamento de Engenharia Mecânica e Industrial
Faculdade de Ciências e Tecnologia, Universidade Nova de Lisboa
Campus Universitário, 2829-516 Caparica
e-mail: dv@fct.unl.pt

[†]Departamento de Engenharia Mecânica e Industrial
Faculdade de Ciências e Tecnologia, Universidade Nova de Lisboa
Campus Universitário, 2829-516 Caparica
e-mail: {deric, ajb}@fct.unl.pt

**Key words:** Bridge Aerodynamics, Bridge Deck, Box-Girder, Spalart-Allmaras, Galloping.

**Abstract.** *This paper deals with a computational study of the aerodynamics of a generic bridge deck section under the action of lateral wind. The bridge section consists of a wide, thin deck on top of a girder box that has a shape close to a rectangle. In the prototype, the borders of the deck are shored by relatively slender beams, placed diagonally, and supported near the base of the girder box. Two two-dimensional, steady-state situations are addressed: section without shoring beams and section with solid panels along the plane of the shoring beams. The aerodynamic coefficients for drag, lift and moment are obtained for angles of attack in the range of −8° to +8°. The den Hartog criterion for galloping is also addressed. The code Fluent is used with the Spalart-Allmaras model for turbulence. The results for the first configuration show that a number of recirculation zones are formed below the deck, which have a large impact on the wind loading of the bridge. Lining the shoring with panels considerably reduces the importance of these recirculation zones, and the aerodynamic coefficients exhibit a more favourable trend against the angle of attack. Therefore, this geometry modification can be considered as a means of improving the aerodynamics of bridges without any major change to their structural design.*

## 1 INTRODUCTION

Because of technical and scientific advances (including new design tools and materials), economic development, and transport volume, bridges are now being built where they could not before. This means they are getting higher or longer. In particular, the span of cable-stayed box girder bridges is getting longer. Under certain conditions [1], such as when the span of the bridge and/or height of the pylons become large so that the overall rigidity of the structure is reduced and the fundamental frequency is lowered, the bridge becomes prone to vibration. Then, it is important to carefully address the effects the wind may have on the deck. In particular it needs to be checked if the flow pattern established by the wind around the deck can excite a mode of vibration of the whole bridge, for example through vortex shedding or flow separation and reattachment. Structural damage can result on the bridge if it experiences strong vibration. A bridge requiring such an aerodynamic study will be built soon in the north of Portugal. This is a cable-stayed bridge with a concrete box girder deck. It is for road traffic and has four lanes.

The research group for aerodynamics of the Department of Mechanical and Production Engineering (Faculdade de Ciências e Tecnologia, Universidade Nova de Lisboa) became in charge of performing wind-tunnel tests of that bridge's deck. To this end, a scaled-down sectional model of the deck has been constructed, and is described in Section 2.

The present computational study has been motivated by the need to better understand the flow pattern around the experimental model to facilitate the interpretation of the experimental results. Indeed, it is quite straightforward to obtain the flow pattern map (in terms of recirculation zones, stagnation points, streamlines) with the CFD tool once the solution has been reached, while it would be much more laborious and time consuming to do the same experimentally.

This is the first part of a more extensive computational and experimental study. This means that even though the final objective will be to study the dynamic response of the bridge to lateral wind, the work reported here is restricted to a stationary model. Hence, forces induced by deck motion cannot be accounted for and the results are valid as long as stationary aerodynamics holds. Also, it should be noted that the computational study refers to the scaled-down experimental model and not to the full scale bridge. Moreover, the study concerns the bare model, i.e. that without any safety-barriers on the deck.

After attending to the situation corresponding to the experimental case, the computational study has been taken further to consider a geometry modification that could possibly lead to improved aerodynamics of the deck. We decided to adopt a modification that does not imply any change whatsoever to the structural part of the section but rather consists of an add-on to the deck.

Both situations are studied for various angles of attack ($\alpha$) in the range of $-8°$ to $+8°$ (positive angles correspond to the windward border of the deck up). Recirculation zones are identified and the static aerodynamic coefficients for drag, lift and moment are obtained. The den Hartog criterion for galloping is also briefly addressed.

## 2 BRIDGE DECK GEOMETRIES

### 2.1 Original, open deck

The bridge section consists of a wide, thin deck on top of a girder box that has a shape close to a rectangle, see figure 1a. In the prototype, the borders of the deck are shored by relatively slender beams, placed diagonally, and supported near the base of the girder box. These beams are evenly spaced along the length of the bridge, with the

modulus being 7.5 times grater than their width. This allows the beams to be safely neglected in order to carry out a two-dimensional computational study, see figure 1b. This can still provide good insight into the aerodynamics of the bridge deck because, as will be seen later in the results, the beams remain totally within recirculation zones featuring low velocities. The chord and height of the model are, respectively, $d$=420 mm and $b$=53.8 mm.

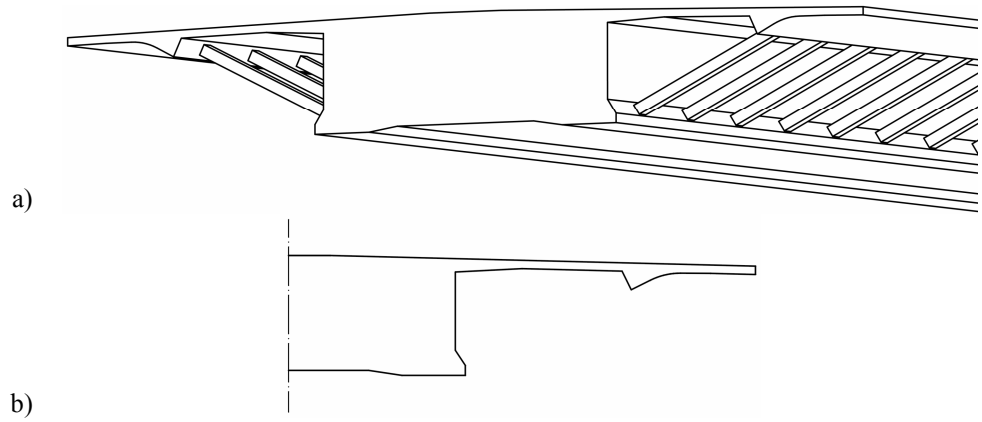


Figure 1: a) perspective of the sectional model of the original bridge's deck; b) simplified section for the two-dimensional numerical study.

## 2.2 Modified, closed deck

In the second situation, the bridge section becomes closer to a trapezoid by using panels fixed to the shoring beams. These panels are shown in light grey in figure 2a. This is a more streamlined section for lateral wind. It is similar to that of the Sunshine Skyway Bridge (Tampa Bay, Florida), completed in 1986, that has been performing well under wind action [2]. This solution of adding panels, should it become necessary, would not involve, in principle, major changes to the structural project of the bridge. The study of this geometry modification is of significance because it is worth being considered should it become necessary to improve the aerodynamics of the bridge. This geometry too can be address as two-dimensional geometry, see figure 2b.

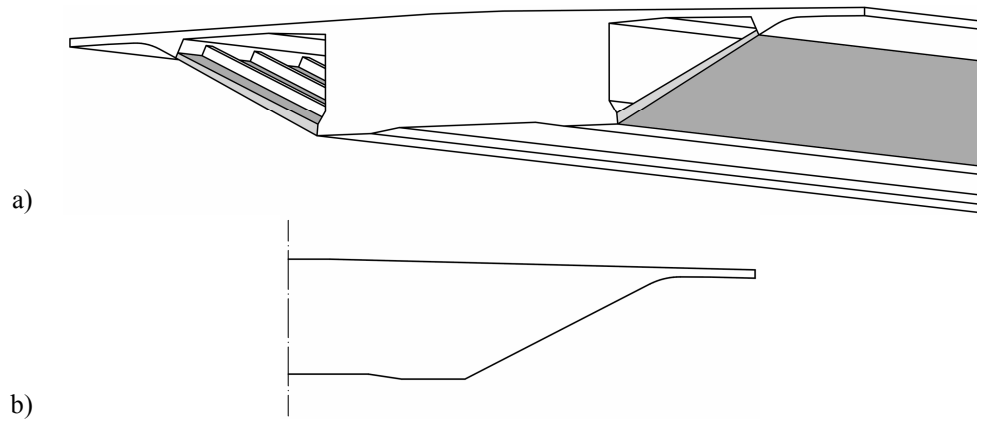


Figure 2: a) perspective of the bridge's model after being modified by the addition of panels enclosing the anchors; b) simplified section for the two-dimensional numerical study.

# 3 CASE SET-UP

## 3.1 Solver and discretization of the equations

The numerical simulations are carried out using version 6.3.26 of FLUENT-ANSYS [3]. The FLUENT code is based on the finite volume method with unknowns, like velocity and pressure, located at the center of the elemental control volumes. The present computational study refers to two-dimensional domains.

Unsteady RANS equations are solved, to attain a steady final solution. This approach was necessary since, for the geometry under study, the steady RANS model produced unrealistic results. Time integration is carried out in a second order implicit scheme.

Closure is achieved using the Spalart-Allmaras turbulence model [4]. This one equation model is known for offering a reasonable balance between computational efficiency and accuracy in simulating the flow around streamline bodies. When experimental data becomes available we shall compare results obtained with other turbulence models as well.

The fluid around the model is air and has been considered as incompressible. The standard second order pressure scheme is used for the pressure term of the RANS equations and the convective term is discretized using a second order upwind scheme. The differencing scheme is used for the diffusion term in the equations. The coupling between pressure and velocity is achieved by the SIMPLEC algorithm.

No problems have been encountered in the convergence of the iterative process, with the under-relaxation factors set to 0.3 for pressure and to 0.7 for momentum.

## 3.2 Domain discretization and boundary conditions

As described in section 2, two two-dimensional situations are addressed: an ‘open’ section and a ‘closed’ section. The two computational cases are set-up in essentially the

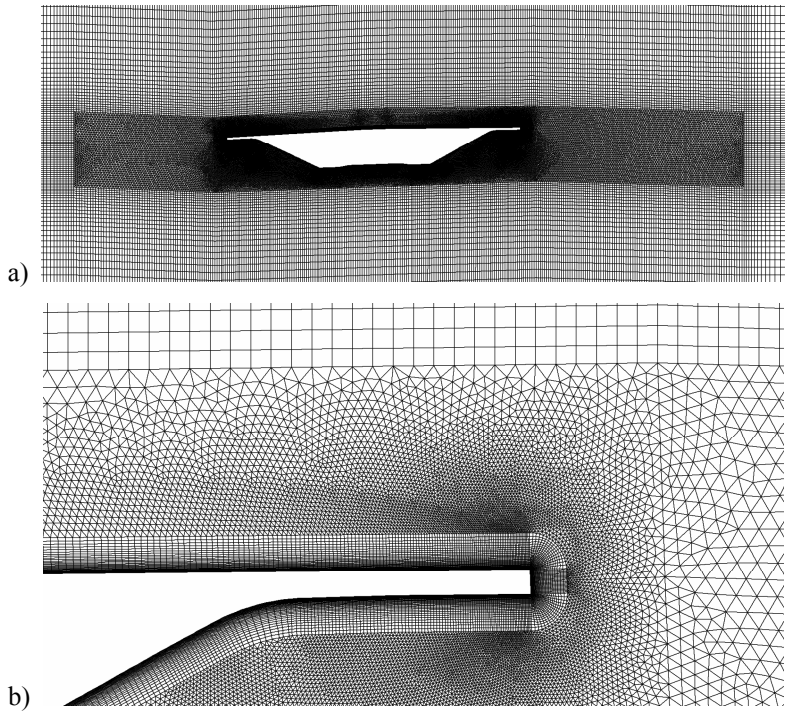


Figure 3: Example of the mesh (partial views of the domain for the ‘closed’ configuration, $\alpha = -2°$):
a) whole section of the model and the extension of the region where triangular cells are used;
b) detail of the downwind border showing the layers of rectangular cells used in the discretization of the boundary layer.

same way except for the comprehensible difference in the number of cells used in the discretization of the domain: 265 000 in the 'open' configuration and 195 000 for the 'closed' one. The mesh is composed of mixed cells, triangular and rectangular, as can be seen in figure 3.

The deck section is at the center of a large rectangular domain, with a height of about 440 times that of the deck. This way, the top and bottom boundaries are located sufficiently far from the model to reduce the numerical blockage effect.

Figure 3b shows the mesh in the close vicinity of the downwind border of the deck. Triangular cells are used in the region close to the model with their areas reduced in the direction of the solid body in order to correctly capture the velocity profile. However, layers of rectangular cells have been preferred adjacent to the solid wall in order to achieve a good dicretization in the normal direction. These layers are in a number and up to a height that allows to directly simulating the viscous boundary layer. Hence, no wall function is used. The height of the first layer of cells is such that, for the given bulk velocity of the flow, a typical value of around 0.6 is found for the dimensionless parameter $y^+$.

Boundary conditions have been set as follows. The upstream velocity of the air is $U_\infty = 10$ m/s and horizontal (thus, $V_\infty = 0$ m/s) and there is no turbulence at the inlet (the modified turbulent viscosity is $10^{-6}$ $m^2s^{-1}$). At the outlet, the outflow condition [3] is specified. The top and bottom boundaries are walls with slip condition whereas the no-slip condition is specified over the surface of the bridge deck model.

## 4 RESULTS AND DISCUSSION

### 4.1 Aerodynamic coefficients

After a steady solution has been reached for a set of angles of attack (α), pressures on the bridge deck surface are integrated along its contour to yield the aerodynamic drag ($D$), lift ($L$) and moment ($M$, defined positive when acting towards increasing a positive angle of attack). The aerodynamic coefficients, per unit length in the spanwise direction, are defined as usual:

$$C_D = \frac{D}{\frac{1}{2}\rho U_\infty{}^2 (b.1)} \qquad C_L = \frac{L}{\frac{1}{2}\rho U_\infty{}^2 (d.1)} \qquad C_M = \frac{M}{\frac{1}{2}\rho U_\infty{}^2 (d^2.1)} \tag{1}$$

Figures 4 and 5 show the results for the 'open' and 'closed' configurations, respectively. In the range $-4° < \alpha < +8°$, the general trends in the curves are similar between the two configurations, apart from a few quantitative details to be discussed further below. In this range the curves have the typical shapes for such slender an object immersed in a flow. In particular, the drag coefficient curves exhibit a local minimum when the body is fairly aligned with flow: about $C_D = 0.78$ for $\alpha = +1.5°$ for the 'open' configuration and $C_D = 0.40$ for $\alpha = -1°$ for the 'closed' configuration. Up to about +5° the lift coefficient, $C_L$, increases almost linearly, with a slope of 0.06 per degree for the 'open' configuration, and 0.10 per degree for the modified configuration. Zero lift is observed at −1.4° for the 'open' configuration while for the other it occurs at almost zero angle of attack (about +0.3°). Moment is bounded between −0.18 and 0.14 for both configurations, and seems to be related to the symmetric of $C_L$. $C_M(\alpha)$ crosses the α axis at −5.4° and −2.8° for the original and modified configurations, respectively.

The two sets of curves become substantially distinct for angles of attack below −5°. While the curves for the 'closed' deck case continue with the trends that have been described above, those for the 'open' deck configuration exhibit a rather sharp change in behaviour when the angle of attack is varied from −5° to −6°. Indeed, drag and lift coef-

ficients are substantially reduced from 0.98 to 0.65 and from −0.25 to −0.55, respectively. In turn, $C_M$ becomes positive as α is decreased from −5° to −6°. This is better explained by observing and interpreting the changes in flow pattern as the angle of attack is varied. This is done later, in section 4.2 below.

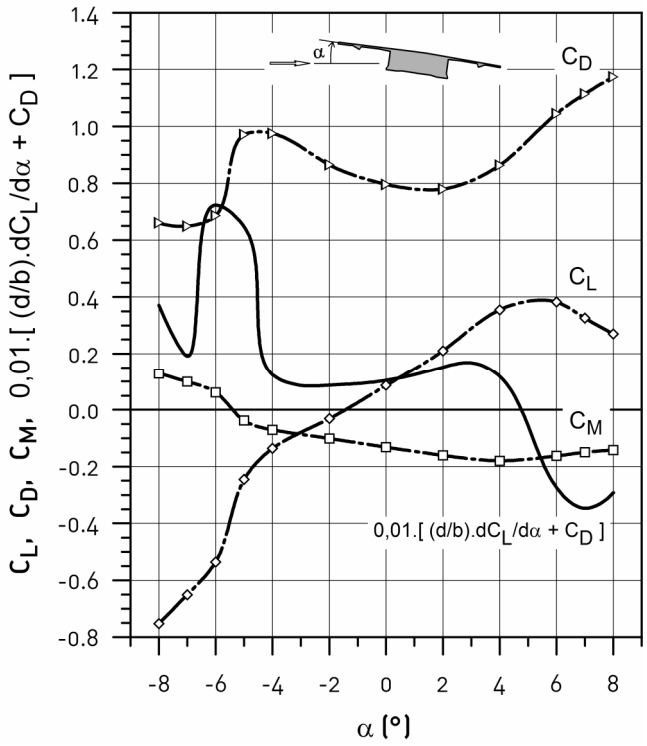


Figure 4: Aerodynamic coefficients for the 'open' configuration of the bridge's deck as a function of angle of attack.

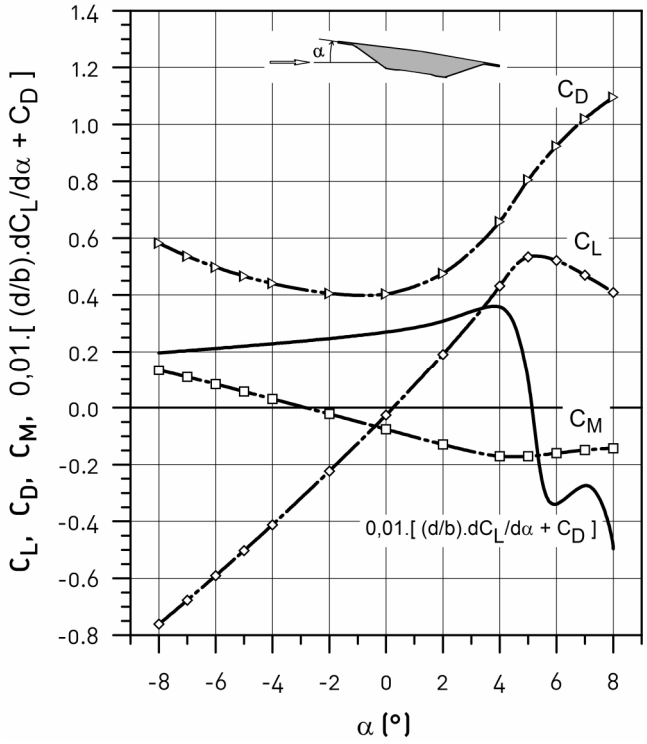


Figure 5: Aerodynamic coefficients for the 'closed' configuration of the bridge's deck as a function of angle of attack.

In the experimental trials for the 'open' configuration at α=-5°, $U_\infty$ has been varied significantly and an accompanying (small) dispersion of the values of $C_D$ has been observed. This suggests that the condition of 'open' deck at α≈-5° corresponds to a situation of aerodynamic instability. The 'closed' deck configuration however exhibits a monotonic trend in $C_D(\alpha)$ and the values of drag are also consistently below those of the 'open' deck case, over the entire range of angle of attack studied. These results suggest that the addition of panels to the sides of the box girder can improve the aerodynamic behaviour of the bridge deck.

Galloping is a regime of vibration that can occur in long-span box girder bridges, in particular when the deck aspect ratio $d/b$ is smaller than 4.0 [6]. In this case the slope of the $C_L(\alpha)$ curve can happen to be negative for the very small angles of attack typical of the situation of lateral wind over bridges. The deck section at hand has a larger aspect ratio ($d/b$=7.8) and thus galloping could only occur for implausible angles of attack (above that for which the slope of $C_L(\alpha)$ becomes negative in the graphs of figures 4 and 5). Nevertheless, we wanted to appreciate if the addition of the side panels to the deck could have any positive effect in what regards aerodynamic instability by galloping. Therefore, we set ourselves to find out the angle of attack at which galloping could occur for both configurations.

Galloping may occur when the aerodynamic force on the body satisfies the following necessary condition [5]:

$$\frac{dL}{d\alpha} + D < 0 \tag{2}$$

or, using the non-dimensional coefficients defined by equations (1),

$$\frac{d}{b}\frac{dC_L}{d\alpha} + C_D < 0 \tag{3}$$

The left member of equation (3) is plotted on the graphs of figures 5 and 6 (it is the continuous curve without symbols on it). It can be observed that condition (3) is met for α>4.7° for the original deck and for α>5.1° for the deck modified with panels. This is a marginal, though positive, improvement suggesting that modifying the deck section in the way here reported is not the best solution to control the phenomenon of galloping. An approach such as that described by Saito and Sakata [6] could be considered instead.

### 4.2 Mean flow pattern around the deck section

Numerical simulations were performed for a reasonable number of angles of attack, as show in figures 4 and 5, in order to obtain a good description of the curves there depicted. However, the flow pattern is fairly similar among a few sets of α, hence it will not be necessary to exhaustively describe the flow pattern for all the numerical cases carried out. Based on the shape of the drag and lift curves for the 'open' situation, four angles of attack have been selected for discussion here, two negative and two positive: both limits of the range studied, i.e. -8° and +8°, -2° as a small angle typical of the incidence of lateral wind on bridges, and -5° for it is around this angle of attack that the aerodynamic coefficients go through a sharp change in values. The same angles are taken for discussion of the modified deck configuration.

Figure 6 shows velocity magnitude filled-contours and a selection of streamlines for the 'open' deck configuration. Figure 7 shows the same kind of results for the situation in which panels are added to the deck (as depicted in figure 2). In what follows, these results are described and interpreted and possible explanations of the trends in the curves of figures 4 and 5 are put forward.

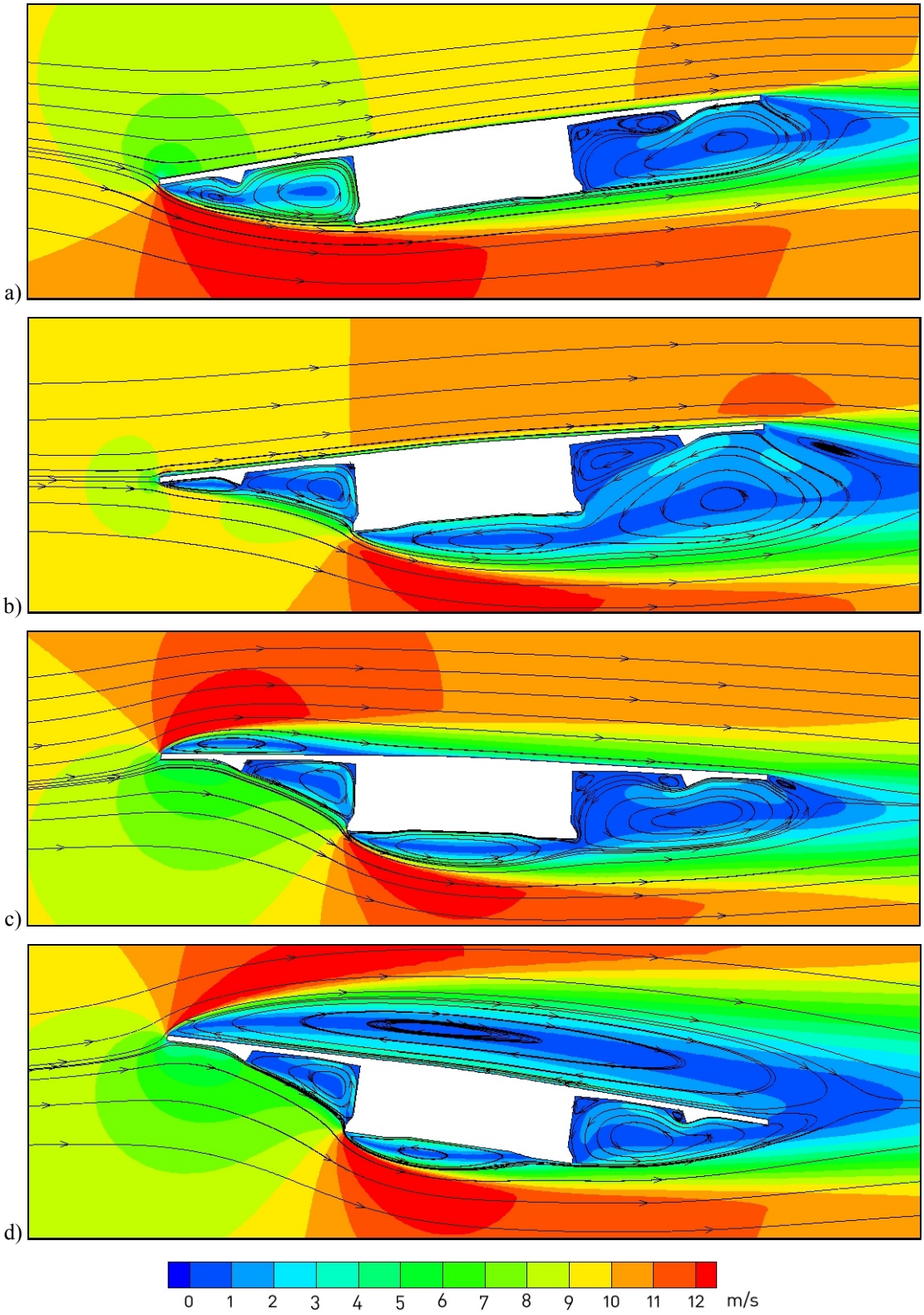


Figure 6: Velocity magnitude contours and streamlines for the 'open' deck configuration at four angles of attack: a) $\alpha = -8°$; b) $\alpha = -5°$; c) $\alpha = +2°$; d) $\alpha = +8°$. Flow is from left to right.

We begin with the 'open' deck configuration, noticing that the rectangular regions corresponding to the sites of the shoring beams remain within the recirculation zones that are established between the borders of the deck and the girder box. This validates the premise on which the two-dimensional simulation of the 'open' deck is based. For all angles of attack recirculation zones are formed both windward and leeward of the

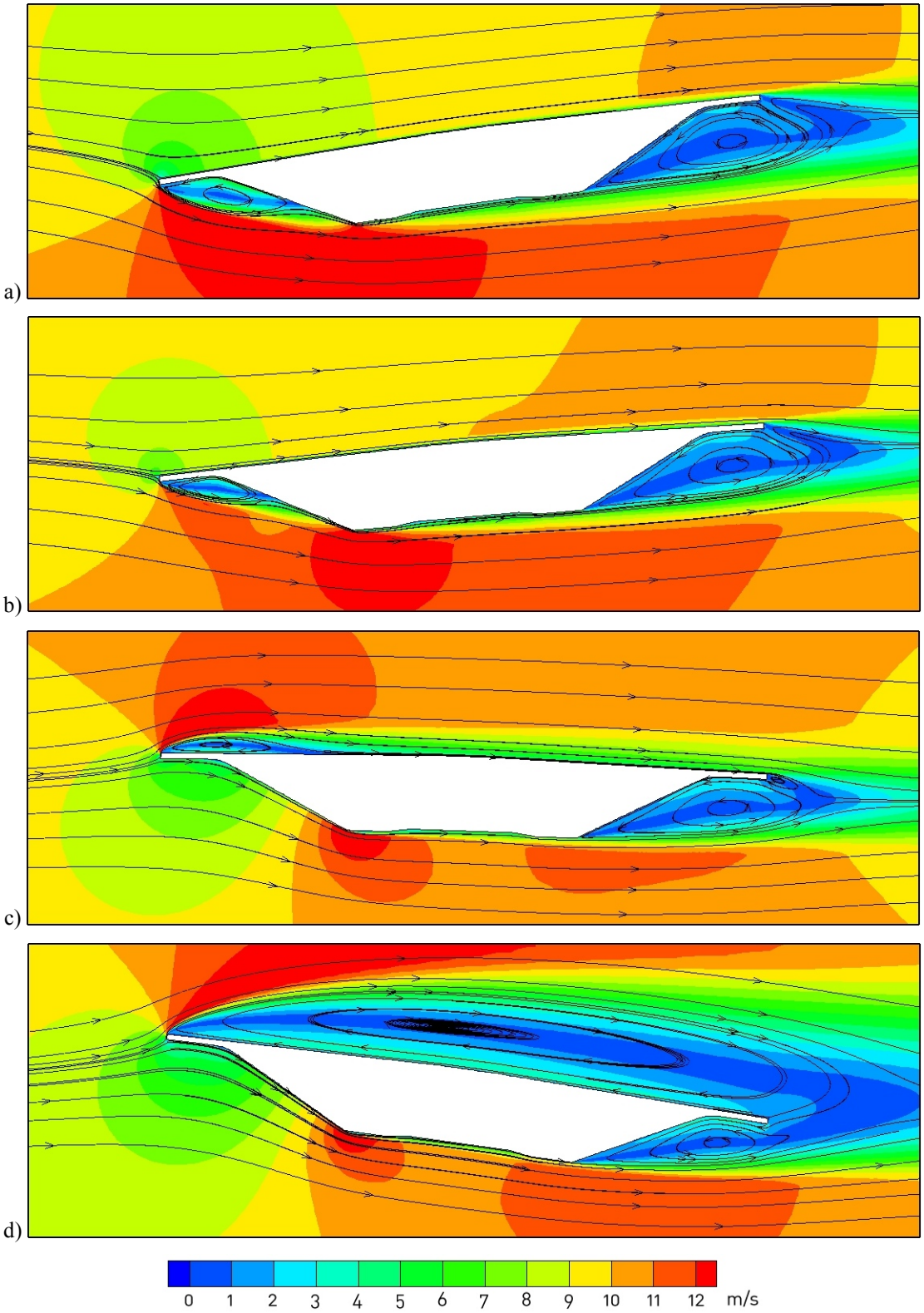


Figure 7: Velocity magnitude contours and streamlines for the 'closed' deck configuration at four angles of attack: a) $\alpha = -8°$; b) $\alpha = -5°$; c) $\alpha = +2°$; d) $\alpha = +8°$. Flow is from left to right.

box girder. The situation $\alpha = -8°$ is the only one, of those depicted, in which the recirculation at the base of the box girder is missing. This is because the windward recirculation zone deflects the mean flow in a way that it becomes aligned with the bottom of the girder. Furthermore, the flow is completely attached to the deck's top. Therefore, this is the most streamlined of all situations and this agrees with the observed lowest value of

$C_D$. The streamline dividing the flow into two parts, one that goes over the deck's flat top and the other that flows under the deck, ends at the top edge of the deck's leading border. For small variations of α the flow will split according to this geometrical criterion, and this explains the fairly constant of $C_D$ up to α=−6°. At α=−5°, the flow no longer divides at that edge and the maximum values of velocity shift from the deck's leading edge to the vicinity of the bottom windward corner of the box girder. A large recirculation zone appears below the girder and, at this angle, it truly interacts with the leeward recirculation zone, forming a large separated region that yields higher drag. As α is increased, the recirculation zone below the box girder becomes thinner while the flow remains attached to the deck's top. As a result, $C_D$ diminishes up to α=+2°. At this angle the flow is splitting at the bottom edge of the deck's leading border. That part of the flow that runs under the deck remains attached to the small length of the deck's border until it meets the recirculation zone leeward of the box girder. However, the top fraction of the flow separates at the leading edge. It reattaches at about a quarter of the deck's chord. Hovering over this recirculation zone is a region of high velocity. As the angle of attack increases, the separated region on the deck's top becomes longer and at around α=+6° (when $C_L$ begins to decrease) the flow is completely separated. Figure 6a depicts this situation for α=+8°. The large trail results in large values of $C_D$.

In what regards the 'closed' deck configuration, one can say that the cavity enclosed by the panels partly substitute the two recirculation zones that have been observed for the 'open' configuration windward and leeward of the box girder. However, the angle of the panels is such that the flow always approaches the bottom upwind corner of the girder at such shallow an angle that no recirculation whatsoever is formed below the girder. The region of high velocities that is formed around that corner becomes substantially reduced. Hence, $C_D$ is overall lower for this configuration. The flow in the neighbourhood of the leading border goes through an evolution similar to that described above for the 'open' deck, with the flow splitting at the top edge for α=−8° and at the bottom edge for positive α. Again, a region of separated flow develops for positive angles of attack on the deck's top. The flow pattern for α=−5° is now similar to that for α=−8°, and the evolution of the aerodynamic coefficients is now almost linear between those two angles (see figure 5).

## 5 CONCLUSIONS

The flow around the stationary model of the deck section of a box-girder bridge has been addressed in a two-dimensional computational study. Two geometries have been considered and are designated as 'open' and 'closed' deck configurations. The curves of the aerodynamic coefficients against angle of attack, in the range $-8° < \alpha < +8°$, exhibit shapes and values typical of such slender sections. However, in the 'open' deck configuration, drag and lift are substantially reduced when α is varied from −5° to −6°. This seems to be related with a shift in position of the stagnation point on the windward edge of the deck, between to positions of local equilibrium, that causes, for angles of attack less negative than −6°, the formation of a recirculation zone at the slightly concave base of the girder. When panels are mounted between the shoring beams, to produce the 'closed' deck configuration, the flow at the windward bottom corner of the girder becomes more aligned with the girder's bottom surface and a recirculation zone no longer develops there, for any angle of attack. Lift and moment show an almost linear variation with α and, most important, drag is substantially reduced. Hence, the addition of panels improves the aerodynamic behaviour of this deck section.

The aerodynamic instability by galloping has been looked into. The large aspect ratio of the deck section implies that if galloping is to occur, it will be for implausible angles

of attack, in the context of lateral wind over bridges. The marginal improvement observed when modifying the shape of the girder with panels indicates that this would not be the best solution to control the phenomenon of galloping.

## REFERENCES

[1] Eurocode 1: Actions on structures – Part 1-4: General actions – wind actions, EN 1991-1-4 (2005)

[2] F. Ricciardelli, On the wind loading mechanism of long-span bridge deck box sections. *J. Wind Eng. Ind. Aerodyn.* **91**, 12-15, pp. 1411-1430 (2003)

[3] Fluent 6.3.26 User's Guide, *FLUENT-ANSYS* (2006)

[4] P.R. Spalart and S.R. Allmaras, A one-equation turbulence model for aerodynamic flows. *AIAA Paper 92-0439* (1992)

[5] J.P. den Hartog, Self Excited Vibrations, Chapter VII of Mechanical vibrations, 3rd Edition, *McGraw Hill* (1947)

[6] T. Saito and H. Sakata, Aerodynamic stability of long-span box girder bridges and anti-vibration design considerations. *J. Fluid and Structures* **13**, pp. 999-1016 (1999)